Green Chemistry

PAPER

View Article Online
View Journal | View Issue

Cite this: *Green Chem.*, 2018, **20**, 2558

Supramolecular double networks of cellulose nanofibrils and algal polysaccharides with excellent wet mechanical properties†

Tobias Benselfelt, * Joakim Engström and Lars Wågberg *

Supramolecular double network films, consisting of cellulose nanofibrils (CNF) entangled with the algal polysaccharides alginate or carrageenan, were prepared using a rapid vacuum filtration process to achieve water-resistant CNF nanopapers with excellent mechanical properties in both the wet and dry states following the locking of the structures using Ca^{2+}. The rigid network of calcium alginate was more efficient than the more flexible network of calcium carrageenan and 10% by weight of alginate was sufficient to form a network that suppressed the swelling of the CNF film by over 95%. The resulting material could be compared to a stiff rubber with a Young's modulus of 135 MPa, a tensile strength of 17 MPa, a strain-at-break above 55%, and a work of fracture close to 5 MJ m^{-3} in the wet state, which was both significantly stronger and more ductile than the calcium-treated CNF reference nanopaper. It was shown that the state in which Ca^{2+} was introduced is crucial, and it is also hypothesized that the alginate works as a sacrificial network that prevents the CNF from aligning during loading and that this leads to the increased toughness. The material maintained its barrier properties at elevated relative humidities and the extensibility and ductility made possible hygroplastic forming into three-dimensional shapes. It is suggested that the attractive force in the CNF part of the double network in the presence of multivalent ions is due to the ion–ion correlation forces generated by the fluctuating counter-ion cloud, since no significant ion coordination was observed using FTIR.

Received 21st February 2018,
Accepted 17th April 2018

DOI: 10.1039/c8gc00590g

rsc.li/greenchem

Introduction

Cellulose nanofibrils (CNF) are composed of crystalline cellulose that forms high aspect ratio fibrils which are the fundamental load-bearing structures in plants. Due to the nanoscale properties and the inherent strength of the cellulose crystal structure, CNF can be used in advanced material applications such as aerogel supercapacitors and sensors,[1,2] conductive materials and printed electronics,[3,4] fire-retardant materials,[5,6] strong and bioactive filaments,[7,8] and nanocomposites.[9,10] The need for a circular economy makes it desirable to use CNF to compete with non-renewable petrochemical raw materials in, for example, the packaging industry.

In order to reach the full potential of CNF there are, however, several fundamental challenges that need to be addressed, one of the most important being the high sensitivity of CNF towards water. Water acts as a plasticizer for polysaccharides such as cellulose and this means that the properties of, for example, a CNF paper (nanopaper) are drastically changed when the material is exposed to liquid water or to moist air.[11]

The preparation of CNF often involves a modification step to introduce charged groups such as carboxylic acids, phosphates, or quaternary amines onto the surface of the CNF to facilitate the liberation of the fibrils from the pulp fiber and to improve the colloidal stability of the dispersion.[12–15] This modification results in an even greater sensitivity to water, as ionic swelling is added to the list of properties of the materials prepared from CNF.

The interaction with water can be an advantage in, for example, liquid storage and biodegradability, but it is in general a disadvantage during the lifetime of the material and especially in the packaging industry, where both the barrier and mechanical properties of the CNF films/nanopapers are

Department of Fibre and Polymer Technology, Wallenberg Wood Science Center, KTH Royal Institute of Technology, 100 44 Stockholm, Sweden.
E-mail: wagberg@kth.se, bense@kth.se

† Electronic supplementary information (ESI) available: A description of the AFM method used to determine the fibril dimensions, descriptions of the ^{1}H-NMR methods used to determine the G/M ratio of alginate and the composition of the carrageenan, information about the SEC method used to determine the molecular weight of alginate and carrageenan, a description of the FE-SEM, a figure showing the histogram of the fibril thickness and an AFM image of the CNF, a figure showing the NMR spectra of ι-carrageenan and κ-carrageenan, a figure showing the FE-SEM image of the cross-section of dry nanopaper, and a figure showing the FTIR data of the different composites. See DOI: 10.1039/c8gc00590g

severely impaired by water. A smart material design is therefore desired in order to make the bio-based materials stable under moist or wet conditions without losing their biodegradability or mechanical properties in the dry state.

Nature has in one way addressed this inherent water sensitivity by the molecular design of polysaccharides, such as alginate and carrageenan, which form structured supramolecular networks in water even though the polysaccharide is highly charged and water-soluble under certain conditions. Many of these polysaccharides are found in plants such as algae or in certain bacteria that grow and live in wet environments, but they are also a common component in the cell wall of most plants in the form of pectin.[16,17] The supramolecular assembly is based on the coordination of free donor electron pairs of oxygen in the polymers with complexing ions to form coordinate bonds (dative covalent) to replace the hydration shell of the ion, and this is a well-known phenomenon of crown ethers,[18] monosaccharides,[19] and proteins.[20] A specific geometry and chemistry is crucial for this coordination to occur, and nature has developed quite complex structures to take advantage of this interaction.

Alginate, extracted from brown algae, is a block co-polymer of L-guluronic acid (G) and D-mannuronic (M) acid in three different types of blocks: GG, MM, and MG/GM, and the composition varies between species and also between the different parts of the plant. The GG block is α-1,4-linked L-guluronic acid which forms a buckled shape that can host multivalent ions, typically Ca^{2+}, to crosslink alginate chains into a strong gel network.[16,21] The first coordination model that is still widely used is the egg-box model from the early 1970s where calcium is hosted in the cavities between two alginate chains with a two-fold helical conformation.[22] Several oxygen atoms on the saccharide rings interact with the calcium ion[16] and a minimum of 8–20 G units in the sequence is required for gelling to occur,[23,24] which shows that both a short-range ion coordination and a long-range order are important for the gel formation. The egg-box model has, however, been challenged, and is not an exclusive explanation for the gel formation of alginates.[25–27]

Several pectin subtypes have the block of α-1,4-linked D-galacturonic acid in common which is a mirror image of the GG-block in alginate at all positions except the C3 position.[28] The buckled structure of alginate and pectin is supposedly designed to host multivalent ions in a cooperative cavity by combining two polysaccharide segments.[28]

Another gelling polysaccharide family is the carrageenan found in red algae. Carrageenan is composed of galactose units and 3,6 anhydrogalactose units linked *via* alternating β-1,4 and α-1,3 bonds and is divided into sub-types depending on the substitution of the sulphate groups.[29] Carrageenan does not have the buckled structure observed in alginate and pectin, but has an advanced two-step self-assembly. The first step is a temperature- and salt-dependent coil to double-helix transition which results in the formation of a soft gel.[30] The double helix arrangement provides a chemically interactive form that can host ions in order to further facilitate a stronger gel formation between the two double helices in a manner similar to that of alginate and pectin gels.[31,32] κ-Carrageenan shows a specificity towards larger monovalent ions from group I and especially potassium, while ι-carrageenan has a favorable interaction with divalent ions and preferably calcium ions.[32,33] The specificity towards potassium is interesting because it should not be able to form purely electrostatic bridges, which have been suggested as an alternative to ion coordination,[34] and this indicates that the gelling mechanism is controlled by specific binding sites.

Oxidized cellulose is in many ways similar to the alginate and pectin structures but does not have the buckled conformation of alginate and pectin or the salt-dependent thermoresponsive assembly of carrageenan. Cellulose is water insoluble and has a crystalline organization in most living plants, but with a high degree of modification it can be soluble in aqueous media. Highly modified cellulose, such as carboxymethyl cellulose (CMC) at a similar degree of substitution (DS) as carrageenan and alginate, is soluble in a high concentration $CaCl_2$ solution which demonstrates that the supramolecular organization of alginate, pectin and carrageenan is crucial for gelling to occur. It has, however, been shown that multivalent ions can have a major impact on the wet stability of nanopapers prepared from CNF with a high concentration of carboxyl groups,[35–37] and this suggests that the organization of cellulose macromolecules into long and stiff nanofibrils influences the interactions between the modified cellulose surfaces in the presence of multivalent counter-ions. The most probable explanation, which will be discussed later in this paper, is that the fluctuating counter-ion density distribution can induce van der Waals-like ion–ion correlation forces when two charged surfaces come close together in the presence of multivalent ions, which is not described by the classical DLVO theory.[38–42]

Alginate and carrageenan are widely used in the food industry as a thickener or gelling agent,[29,43] but recent research has been focused towards biomedical applications.[44] Alginate and carrageenan have earlier been combined with CNF, cellulose nanocrystals (CNC), or bacterial cellulose (BC) which can provide rigidity by acting as a reinforcement in the gel matrix, and it has also been suggested that alginate and CNF or CNC have a cooperative ion complexation.[45–47] In many of these applications, CNF, CNC or BC is added to alginate in an amount of 1–50% before the gelling procedure to form a hydrogel,[45,48,49] aerogel,[46,50] film,[47,51] or fibre.[52,53]

In the present work, CNF has been used as the main component and small amounts (10–30%) of alginate, κ-carrageenan or ι-carrageenan have been distributed in nanopapers by mixing the components in the dilute state followed by vacuum filtration. The anionic nature of both the marine polysaccharides and nanocellulose facilitates a homogeneous mixing of the components, which is almost impossible to achieve with oppositely charged or uncharged systems. These dense and homogeneous composites can subsequently be exposed to different mono- and multivalent ions to lock the network into a material that shows synergetic effects similar to

those found in a double network hydrogel, which has been thoroughly summarized by Chen *et al.*,[54] where alginate works as the tight and brittle sacrificial network that can dissipate energy and CNF works as the long-distance load-transferring network that provides toughness.[55,56] The cooperativity between the two networks and the nature of the network formation with multivalent ions have been investigated.

The approach of blending the components in a non-interacting state and drying the material, followed by a post-treatment to change the properties of one or more components is intriguing from a material design point of view and has been shown to be effective.[57] The wet and dry properties of the alginate/CNF composite nanopapers show that this is a promising approach towards the manufacturing of composite nanocellulose materials with high wet toughness and dry stiffness.

Experimental

CNF preparation

The 2 wt% CNF gel was kindly provided by Innventia AB (now RISE Bioeconomy), Stockholm, Sweden. The CNF was derived from a dissolving grade pulp that had been carboxymethylated to a charge density of 600 ± 50 μmol g^{-1} prior to defibrillation, according to an earlier described procedure.[58] The dissolving pulp from Domsjö Fabriker AB (Aditya Birla) has a hemicellulose content of 4–5 wt% and a lignin content of 0–1 wt%, but it is likely that the residual hemicelluloses and lignin are further solubilized and removed during the carboxymethylation.[58] The gel was further homogenized using a microfluidizer by three passes through a serial 200–100 chamber configuration, diluted to a dry content of 0.2 wt% at a volume of 900 mL, and dispersed using an Ultra-Turrax at 13 000 rpm for 20 minutes. The gel was centrifuged at 4100*g* for 1 h to remove the larger aggregates and flocs. The dimensions of 250 fibrils were measured using atomic force microscopy (AFM) according to the ESI† and the distribution is shown in Fig. S1.† Lengths between 100–1200 nm were observed.

Algae polysaccharide preparation

A solution of alginic acid sodium salt from giant brown algae (high viscosity, Alfa Aesar) was prepared by overnight dissolution with mild stirring at a concentration of 0.25 wt%. The alginate contained an insoluble fraction of approximately 15 wt% that was removed by filtration through a 5 μm syringe filter (Acrodisc, Supor membrane, Pall) and no aggregates were observed with an optical microscope after the filtration. The G/M ratio was estimated using ^{1}H-NMR[59] and showed a G content of 41% and a M content of 59% distributed into blocks of 27% GG, 28% MG, and 45% MM, which are reasonable values according to earlier reports.[52,53] The details of the ^{1}H-NMR measurement are found in the ESI.†

Kappa (κ) carrageenan (Sigma Aldrich) and iota (ι) carrageenan (Sigma Aldrich) were dissolved overnight at a concentration of 0.2 wt%. The composition was determined using ^{1}H-NMR and the integral comparison of the peaks[60] shows that the ι-carrageenan contained 22% κ-carrageenan and 12% contamination, which might be λ-carrageenan or floridean starch,[61] while the κ-carrageenan contained 12% ι-carrageenan. The details of the ^{1}H-NMR measurement are found in the ESI† and the spectra are shown in Fig. S2.†

Table 1 Size-exclusion chromatography data showing the relative molecular weight distributions of the algal polysaccharides

Sample	Relative M_w (kDa)	Relative M_n (kDa)	PDI
Alginate	1209	645	1.88
κ-Carrageenan	1193	733	1.63
ι-Carrageenan	995	417	2.39

The molecular weights of the alginate and carrageenan were characterized by size-exclusion chromatography described in the ESI† and the results are given in Table 1. The molecular weight of ι-carrageenan was stated by the supplier to be M_n between 193 and 324 kDa and M_w between 453 and 652 kDa. The relative M_n and M_w values in Table 1 show that the carrageenan subtypes were similar in terms of weight average but that ι-carrageenan had a larger fraction of lower molecular weight polymers. It should be noted that all the samples were at the limit of both the column and the pullulan standard and the figures given should be considered more as a comparison and as an indication of the dispersity rather than as exact values. The polyelectrolyte effect of these polysaccharides makes them appear larger in SEC and it is important that the molecular weight is considered only as a value relative to pullulan, which is probably why it differs from the value given by the supplier.

Preparation of composite CNF/algae polysaccharide films

CNF was mixed with 0, 10 or 30 wt% algal polysaccharides using an Ultra-Turrax for 9 min at 9000 rpm. The dispersion (400 mg dry weight) was filtered through a Durapore membrane filter (PVDF, Hydrophilic, 0.65 μm) in a Kontes microfiltration assembly with a filter diameter of 8 cm. The filtration time varied between 9 and 36 h depending on the fraction of the algal polysaccharide required to produce the composite films. The retention was determined by measuring the dry content of the filtrate and was greater than 90% for the alginate, greater than 80% for ι-carrageenan, and greater than 70% for κ-carrageenan. The 1–2 mm thick wet gel that was formed after the filtration was dried for 20 min at 93 °C at a reduced pressure of 95 kPa using the drying section of a Rapid-Köthen sheet former (Paper Testing Instruments, Austria). Dry nanopapers with a thickness of 50–60 μm were either conditioned at 50% RH and 23 °C before tensile testing or soaked in solutions of 1 wt% $CaCl_2$ (>97%, Sigma Aldrich), KCl (>99%, Sigma Aldrich), $Cu(NO_3)_2$ (>99%, Sigma Aldrich) or $NdCl_3$ (>99%, Sigma Aldrich) for 24 hours, rinsed in Milli-Q for 24 hours, dried in the Rapid-Köthen or tested in the wet state. An illustration of the preparation procedure is shown in Fig. 1.

Pristine nanopapers were hot-pressed at 150 °C for 1 h at a pressure of 20 kN. The nanopaper turned yellow-orange and it is believed that covalent crosslinking was created through

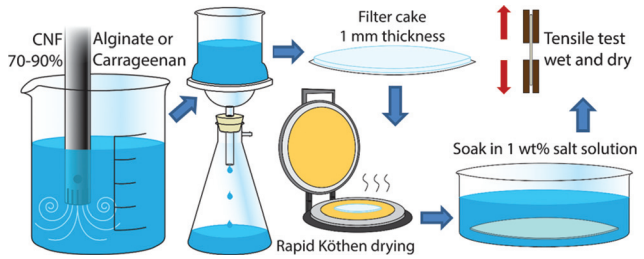

Fig. 1 Illustration showing the method of preparation of the nanopaper composites including: a mixing step, a filtration step, a drying step, and a post-treatment step with different ions by soaking the dried film.

esterification with this treatment.[62] This sample was used as a reference for a covalently crosslinked nanocellulose network.

The pristine alginate reference was solvent-cast under ventilation at ambient temperature over a period of 7–10 days starting with a 0.4 wt% solution.

The dried films were further characterized using Fourier-transform infrared spectroscopy (FTIR) with an attenuated total reflectance add-on (PerkinElmer Spectrum 2000) to investigate the shift of the carboxylate peak positions, which is an indication of the existence and type of ion coordination.

Relative swelling thickness

The nanopaper samples were left to swell in Milli-Q or 1 wt% salt solutions for 24 hours followed by 24 hour rinsing with Milli-Q water and the thickness (d) was measured after the surfaces had been dabbed with fine tissue to remove excess water. The nanopapers exhibited a unidirectional swelling in the thickness direction, and the thickness was used as an easy way to study the wet-integrity. The relative swelling thickness was calculated using the equation:

$$\Delta d = \frac{d_{\mathrm{wet}} - d_{\mathrm{dry}}}{d_{\mathrm{dry}}} \quad (1)$$

where d_{wet} and d_{dry} are, respectively, the wet and the dry thicknesses.

Tensile testing

The samples were cut into pieces of 50 × 3 mm with a reinforced razor blade (no. 743, VWR). The samples were clamped with a gauge length of 20 mm in an Instron 5944 with a 500 N load cell and were strained at a rate of 2 mm min^{-1}. The modulus was calculated as the slope of the curve between the strains of 0 and 0.3%. In the case of the wet samples the linear region between 0–0.15% was used to calculate the modulus. For each composite, 7 to 10 samples were tested and the average modulus, strain-at-break, tensile strength, and work of fracture were calculated with 95% confidence intervals.

Oxygen permeability

The oxygen permeability was measured for a sample area of 5 cm^2 using a MOCON (Minneapolis, MN, USA) OX-TRAN 2/21. The measurements were performed symmetrically with the same relative humidity of 52–53% or 81–82% on both sides of the sample at 23 °C. Two measurements were made for each sample.

Quartz crystal microbalance with dissipation (QCM-D)

QCM-D was used to probe the interactions between CNF and alginate. Detailed information about the technique can be found elsewhere.[63] TEMPO (2,2,6,6-tetramethyl-1-piperidinyl-oxy)-oxidized CNF included in this measurement was prepared according to Saito *et al.*[64] and the dispersions were prepared in a way similar to that used for carboxymethylated CNF. The TEMPO-oxidized CNF was included to investigate if the position of the carboxyl group on the CNF affected the interaction with alginate with or without the presence of multivalent ions, TEMPO forming directly on the C6 of glucose, whereas the carboxymethylated CNF has an ether bond as the spacer between C6 and the carboxyl group. A bilayer of polyethylenimine (PEI) (0.1 g L^{-1}, pH 7.5) and CNF (0.1 g L^{-1}) was adsorbed *in situ* on the QCM crystal to prepare the CNF surface, and the surface was maintained with sodium as the counter-ion or exchanged to calcium counter-ions before the alginate was introduced.

Real-time birefringence during tensile testing

Polarized filters were placed parallel to and at 90° to the strain direction during tensile testing which gives the maximum birefringence when the fibrils are oriented at a 45° angle to the direction of the strain. This makes the measurement more sensitive towards the lower angles of orientation which was expected for this material. The conventional approach would be to place the polarizers at ±45° angle to the strain direction which gives the maximum birefringence for orientation in the direction of the strain.

The alignment of the fibrils towards the direction of the strain leads to interference due to the retardation (Γ) generated by the path difference introduced by the anisotropic refractive index in the cellulose crystal and in the water-filled space between the fibrils. The retardation depends on the thickness of the crystal (d), or in this case the amount of CNF in the thickness direction of the film, according to:[65]

$$\Gamma = d(n_\gamma - n_\alpha) \quad (2)$$

where $n_\gamma - n_\alpha$ is the difference between the light with polarization perpendicular (γ) and parallel (α) to the optical axis of the material. The thickness would in this work be best represented by the thickness of the dry nanopaper.

Hygroplastic forming

The composite films containing 10% alginate were pressed in the wet state into a hemispherical shape as demonstrated earlier by Larsson *et al.*[66]

Results and discussion

Mixing CNF with polymers

The visual appearances of the mixtures of CNF with alginate and CNF with the polycation poly(diallyldimethylammonium

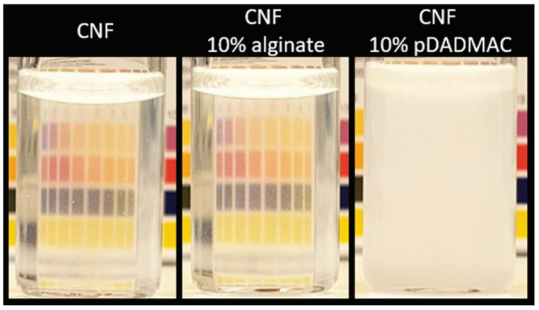

Fig. 2 Visual appearance of a 0.2 wt% CNF dispersion, CNF with 10% alginate, and CNF with 10% pDADMAC.

chloride) (pDADMAC) are shown in Fig. 2. The turbid appearance of the CNF and pDADMAC mixture indicate micron-size aggregates, while the CNF and alginate mixture have the same appearance as the well-dispersed CNF reference. The anionic nature of alginate, carrageenan, and CNF results in stable colloidal dispersions when mixed, which is difficult to achieve with cationic- or interacting uncharged polymers. If successfully mixed with CNF, cationic polyelectrolytes would lock the CNF network through electrostatic interactions to create a water-resistant material, but due to the delicate procedure this is a questionable approach. Aggregated or flocculated CNF lead to an unacceptable inhomogeneity of the assembled material and this affects both the mechanical and optical properties.

When complex polyelectrolyte gels are formed, the aggregation upon mixing can be prevented by adding enough salt to screen the interaction between oppositely charged segments so that they do not associate. The salt can be removed at a later stage to lock the network.[67,68] This is not a feasible route with CNF since the CNF dispersion reaches an arrested state long before the critical salt concentration is attained,[12,13] which makes the mixing of CNF with cationic polymers extremely difficult. The added anionic charge from polyanions, on the other hand, leads to a significantly impaired wet-integrity for the composite, and the addition of anionic polymers which can change properties with a posttreatment when the material is formed, such as alginate and carrageenan, is therefore the preferred way to use polymers to induce wet-stability in the CNF material.

Relative swelling thickness as a tool to investigate the wet integrity of nanopaper composites

Nanopapers containing CNF and 10 or 30 wt% algal polysaccharides were prepared according to Fig. 1 and were then crosslinked with different ions to investigate how the supramolecular structure of alginate and carrageenan affected the dry to wet transition of the nanopaper. The unidirectional swelling of these films meant that it was possible to use the thickness as a quantitative measure of the swelling and a qualitative measure of the wet-integrity, and the swelling data are presented and visualized in Fig. 3.

The differences shown in Fig. 3 can be explained in terms of the equilibrium swelling pressure (Π) of a polyelectrolyte gel

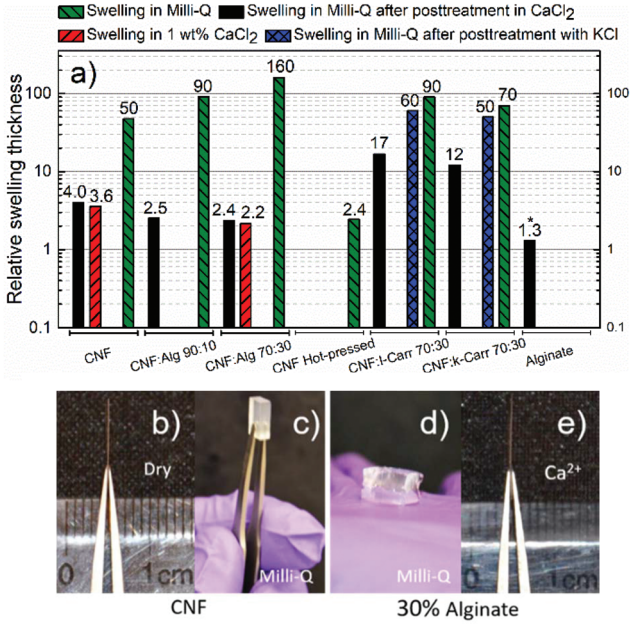

Fig. 3 Swelling of the composite nanopapers showing: (a) the relative swelling thickness, and images of (b) a dry nanopaper, (c) the nanopaper swollen in Milli-Q (50 times the dry thickness), (d) 30% alginate composite in Milli-Q (160 times the dry thickness), and (e) 30% alginate crosslinked with Ca^{2+} (2.4 times the dry thickness). Alg is short for alginate, carr is short for carrageenan, and 90 : 10 or 70 : 30 are the weight mixing ratios. The asterisk indicates that the swelling is not unidirectional in the alginate film.

in order to best interpret the data. The equilibrium swelling pressure can be divided into three contributing parts according to Flory:[69]

$$\Pi_{mix} + \Pi_{net} + \Pi_{ion} = 0 \quad (3)$$

where Π_{mix} is the swelling pressure contribution from the entropy and enthalpy of mixing water and the constituents of the gel, Π_{net} is the pressure of deforming the network which creates resistance to the swelling, and Π_{ion} is the osmotic pressure due to the ionized entities in the gel. At equilibrium, Π is zero, and this means that if Π_{net} is zero the gel is dissolved, and that if Π_{net} is high it may suppress the other contributions so that almost no swelling occurs.

The dry reference CNF nanopaper increased in thickness approximately 50 times when equilibrated in Milli-Q water (Fig. 3a–c) and the main contribution is probably the ionic swelling (Π_{ion}) due to 600 ± 50 μmol g^{-1} sodium carboxylate units in the nanopaper. It has been shown that CNF can have a charge density as high as 1500 μmol g^{-1}, which would result in an even greater sensitivity to water.[15] When the CNF nanopaper was treated with Ca^{2+} ions, almost all the swelling was suppressed, as previously reported by Shimizu *et al.*[35] and this means that the Π_{net} increases and/or that the Π_{ion} decreases when the ion-exchange to the calcium-form induces an attractive force. Similar films prepared from carboxymethylated cellulose (CMC, Sigma Aldrich) with a DS of 0.7 and a molecular

weight of 90 kDa were still soluble in 1 wt% $CaCl_2$, and this suggests that there is a structure in the nanopaper which is not present in the CMC film that is important for the attractive interaction between CNF in the presence of calcium ions.

The incorporation of 10 or 30 wt% alginate or carrageenan into the nanopaper was probably possible through the electrostatic repulsion between the components in the filter cake and the extended conformation of polyelectrolytes in solution, which is indicated by the retention of more than 70–80% of the carrageenan and more than 90% of the alginate. The swelling of 90 or 160 times for the composite with 10 or 30 wt% alginate, respectively, can be explained by the theoretical DS of 1 for alginate that adds an extensive amount of charged groups in the gel and this results in an increased ionic swelling (Π_{ion}) (Fig. 3a and d). The increase in swelling is probably dominated by the increase in the charge density in the film and this makes the swelling proportional to the increased osmotic pressure in accordance with the theory:[69]

$$\Pi_{ion} = \Pi_{osm} = kT\sum(C_{gel} - C_0)_i \quad (4)$$

where $(C_{gel} - C_0)_i$ is the concentration difference of the ion i in the gel (C_{gel}) relative to the surrounding solution (C_0). Crosslinking with calcium ions resulted in the suppression of most of the swelling and to a higher degree than for the CNF reference, which means that a stronger network (Π_{net}) is formed. It was observed that rinsing to remove excess salt lead only to a small increase in thickness, which shows that the osmotic pressure of the counter-ions was almost fully suppressed by the CNF and alginate networks.

A nanopaper was also hot-pressed at 150 °C for 1 hour to produce a reference covalently crosslinked network, which resulted in a yellow color and a wet integrity similar to that of the CNF and alginate composite. It was not possible to detect the cause of the yellow color by FTIR (ESI Fig. S4†), but it has been suggested that the yellow color in dried TEMPO-oxidized materials originates from hemiacetal or hemiketal formation during drying.[70] This suggests that some kind of esterification can occur during the heating of carboxymethylated cellulose, which has been shown between the hydroxyl groups on cellulose and small carboxylic acids, such as hydroxybutyric acid, under similar conditions.[62]

The carrageenan composites without ion coordination exhibited less swelling than the same composition of CNF and alginate with only 90 and 70 times for the nanopapers with 30% ι-carrageenan and κ-carrageenan, respectively. In the case of κ-carrageenan, this can partly be explained by the theoretical DS of 0.5 compared to 1 for alginate and ι-carrageenan, but the degree of ionic swelling for ι-carrageenan should have been greater according to the charge density. This suggests that the network pressure of carrageenan without specific ion involvement is higher than that of alginate due to the thermoresponsive gelling mechanism.

It has been shown that a high concentration of sodium chloride can favor the coil to double-helix transition of carrageenan and allow the thermoresponsive assembly to happen at higher temperatures, which means that carrageenan can be a gel at room temperature without any specific ion involvement.[31,71]

The CNF and carrageenan composite nanopapers were crosslinked with both calcium and potassium ions since the κ-carrageenan has been shown to form the strongest gels with potassium ions, while the ι-carrageenan forms the strongest gels with calcium ions.[72,73] The composites with 30% κ or ι-carrageenan showed a higher swelling ratio than the reference nanopaper in the calcium form (Fig. 3a). The most probable explanation is that the carrageenan gel is not as strong as the alginate, or that the network is not continuous throughout the film. The comparatively high swelling of the calcium-treated carrageenan composites shows that the supramolecular structure of alginate is important and that electrostatic bridges between two anionic charges and one multivalent ion are indeed a questionable explanation.

The swelling of the carrageenan composites was reduced by only 30% in the presence of potassium ions, which shows that the gel network was not strong enough to suppress the swelling of the CNF network, which in turn has no significant attractive interaction in the presence of these monovalent counter-ions. The ion specificity for the ι and κ sub-types could not be clearly distinguished in the swelling and this indicates that the CNF network properties were dominant in these composites.

The efficiency of the calcium alginate network was observed in the swelling of a pristine alginate film by 1.3 times that of the dry thickness. It should, however, be noted that this swelling was not unidirectional as in the CNF films, and this is indicated by the asterisk in Fig. 3a. This also shows that alginate can form dense crosslinked films when soaked in a $CaCl_2$ solution from the dry state.

Mechanical properties in the wet and dry states

The mechanical properties of the composites were measured in both the wet (Fig. 4) and the dry state (Fig. 5). It was observed that a relative swelling thickness of 6–7 was close to the limit of what was feasible for a reliable tensile testing since the highly swollen samples were too weak to maintain their structural integrity in the clamped areas, and hence it was possible to evaluate only the calcium-ion-treated reference and the alginate composites in the wet state using this approach.

Fig. 4a shows that the calcium-treated nanopaper had a significant wet strength with great extension before failure, but was not as stiff as the calcium-treated pristine alginate film. The combination of CNF and alginate showed significantly better properties than would have been expected for a proportional combination of the material properties of the individual components. This indicates that CNF and alginate form an interpenetrating network similar to that reported for double polymer networks.[55,56] When 10% alginate was added, both the modulus and the tensile strength were more than doubled and the material was able to resist a strain above 50% before failure and a work of fracture close to 5 MJ m^{-3} (Fig. 4a–c), which is indeed comparable to a stiff and tough rubber. Shimizu *et al.*[35] studied the crosslinking of nanopapers

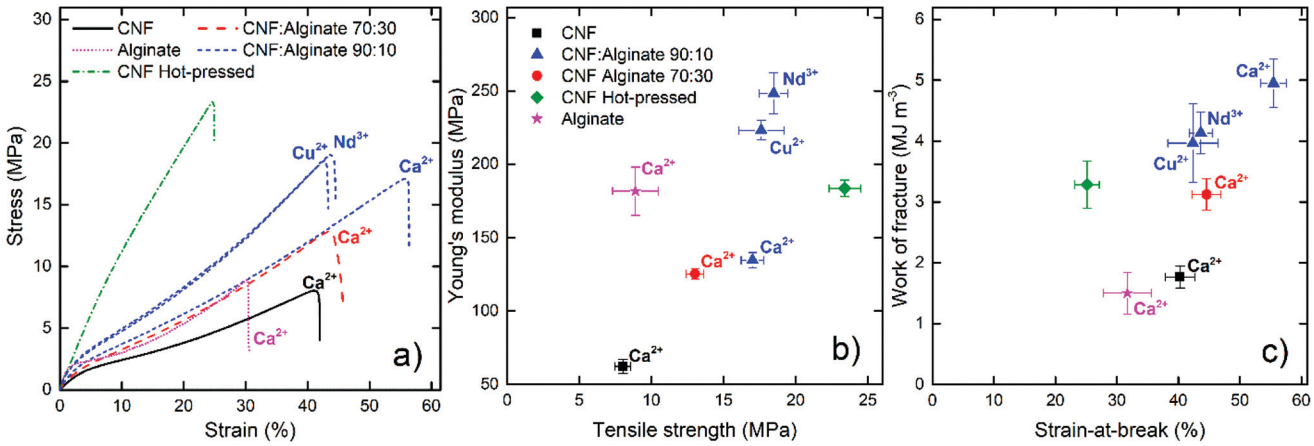

Fig. 4 Wet tensile properties of the prepared composites and of the reference materials showing: (a) representative engineering strain–stress curves, (b) Young's modulus as a function of tensile strength, and (c) the work of fracture as a function of the strain-at-break. The composites were soaked in Milli-Q water for 24 hours prior to testing. The notations close to the curves indicate the crosslinking ion. The error bars are 95% confidence intervals.

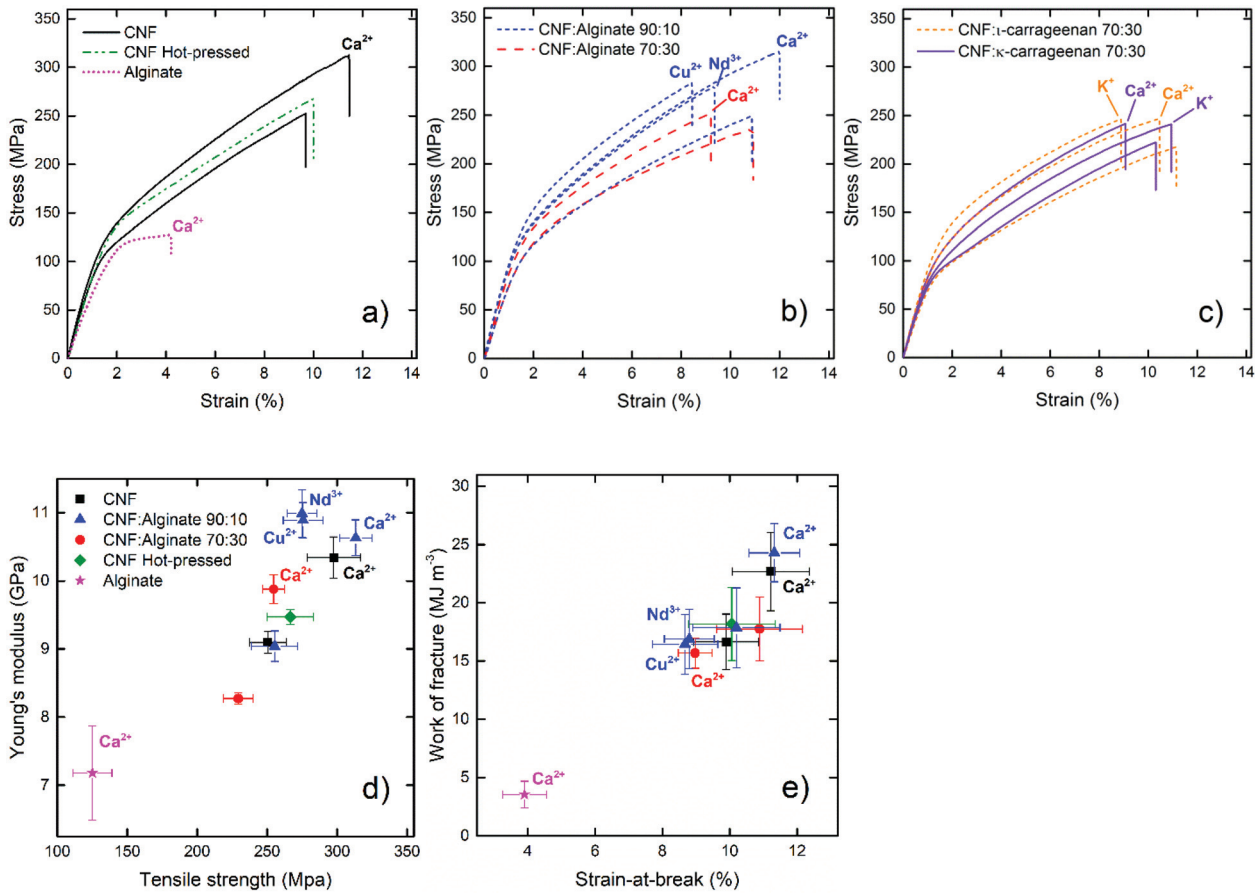

Fig. 5 Dry tensile properties of the composites and of the reference materials showing: (a)–(c) representative engineering strain–stress curves (d) Young's modulus as a function of tensile strength (carrageenan excluded), and (e) the work of fracture as a function of the strain-at-break (carrageenan excluded).

with different multivalent ions to produce stiffer materials without any significant plastic deformation and with a highest toughness of only 1 MJ m^{-3} in the calcium form.

Sun *et al.*[56] have suggested that unzipping of the egg-box structure can dissipate large amounts of energy and that this was the reason for the toughness of the double network hydro-

gels in their work. A similar explanation to the improved toughness for the CNF alginate composite is reasonable. It is also possible that the egg-box regions can break and momentarily reform when a more oriented structure is formed during straining. The data in Fig. 4 suggest that small amounts of alginate can form a fine network between the CNF to transfer loads over a greater distance, but a larger amount of alginate (30%) will disrupt the CNF network to some degree and make the material more similar to the more brittle alginate gel.

The hot-pressed nanopaper was used as a reference covalently crosslinked CNF network and had properties similar to those achieved by multivalent ions in highly charged nanopapers.[35] The deformation mechanism was also quite different from that of the alginate composites; the hot-pressed nanopaper showed a linear deformation while the supramolecular crosslinked composites showed three different regions: a short elastic region, a plastic region, and a strain-induced stiffening probably due to an increased orientation of the fibrils.[74]

Copper and neodymium ions were also tested as the crosslinking agent for the composite films to investigate if the wet strength could be further improved. The results showed a significant stiffening at the cost of a deterioration in the strain-at-break. It has been shown that copper is the divalent ion with the highest affinity towards alginate and that it can interact with all the blocks.[34] Neodymium ions have also shown interesting interactions with alginate to form layered structures with a high dry strength.[75] The crosslinking of the MM and the MG/GM blocks would result in a stiffer network, but the relative swelling thickness of these films was still around 2.4 to 2.5 which appears to be a limit for these composites, regardless of the type of crosslinking ion.

The mechanical properties of the composites were also tested at 23 °C and 50% relative humidity (Fig. 5) to ensure that the increase in wet stability was not achieved at the cost of a decrease in dry strength. The addition of polymers to nanopapers usually leads to a loss of stiffness while extensive crosslinking makes the material stiffer but at the same time more brittle.[76,77] The addition of 10% alginate did not affect the dry material properties significantly and, when the nanopapers were crosslinked with calcium, both the pristine CNF and the 10% alginate composite showed an increase in stiffness and in the strain-at-break with a modulus around 10.5 GPa, a tensile strength above 300 MPa, and the work of fracture approaching 25 MJ m^{-3} (Fig. 5a–b, d and e.), which are impressive properties in terms of un-oriented nanopaper composites that rarely reach strengths close to or above 300 MPa at 50% RH.[76] The 30% alginate composite and the crosslinking with copper or neodymium ions, however, resulted in stiffer and more brittle materials in the dry state.

Large differences were observed in the yield stress of the different composites from roughly 80 MPa for the carrageenan composites, to 110–120 MPa for the references without multivalent ion treatment, and to roughly 150 MPa for the stiffest Cu^{2+}-treated composite. The data show that adding small amounts of alginate with a subsequent crosslinking with calcium ions resulted in a stronger material in both the wet and dry states and that calcium is a favorable ion to form systems with both increased stiffness and increased toughness. The most dramatic improvement was, however, found in the wet state.

The specific gelling ions for the carrageenan, Ca^{2+} for ι-carrageenan and K^{+} for κ-carrageenan, resulted in an increase in the stiffness while at the same time maintaining the strain-at-break, whereas the least favorable gel-inducing ion only increased the stiffness (Fig. 5c). This can probably be explained by the supramolecular structure of carrageenan inside the nanopaper. The carrageenan composites did not reach a dry strength above 250 MPa and were inferior even to the calcium-treated reference nanopaper in the wet state, which shows that carrageenan will not improve the nanopaper in either the dry or the wet state with this approach.

Oxygen permeability

Fig. 6 presents the oxygen permeability data at 50 and 80% relative humidity, and shows that the Ca^{2+} treated composite with 10% alginate was a slightly better barrier than the reference CNF or the calcium-treated CNF at 50% relative humidity, probably because the flexible alginate makes the material denser and more uniform. At 80% relative humidity the permeability of the CNF sample increased drastically, whereas the calcium-treated nanopapers were slightly more stable. The observed oxygen permeabilities between 6–12 mL μm m^{-2} day^{-1} kPa^{-1} can be compared to those of a polyethylene terephthalate (PET) film at around 25–30 mL μm m^{-2} day^{-1} kPa^{-1}.[78]

A low oxygen permeability is an important feature of packaging materials and it is proportional to the accessible free volume in the material. The swelling of bio-based materials due to moisture sorption therefore drastically reduces the barrier properties, as oxygen transport in water is relatively fast. Both multivalent ions[35] and covalent crosslinking[77] can prevent the swelling and maintain the gas barrier properties, and it was therefore interesting to clarify how the alginate composites would behave in this respect. The absolute values are not as impressive as those reported by Shimizu *et al.*[35] or

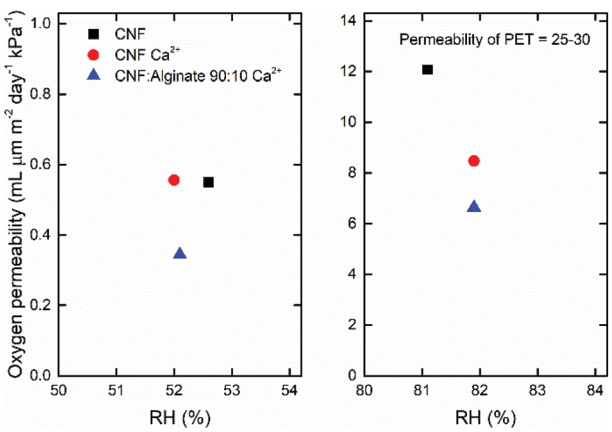

Fig. 6 The oxygen permeability at ~50% RH (left) and ~80% RH (right). The values are the mean of two measurements with a coefficient of variation of less than 12%. The PET reference is for an oriented PET film.[78]

Larsson *et al.*,[77] but for their highly crosslinked nanopapers the improved barrier properties were associated with a high brittleness in the dry state, which is not the case for the composite in the present work.

Cooperative interactions between CNF and alginate networks?

Table 2 shows the FTIR data of alginate, CNF, and the 30% alginate composite in this work, based on the ESI (Fig. S4†), with a band-narrowing ($\Delta\Delta\nu$) between the asymmetric (~1600 cm^{-1}) and symmetric (~1400 cm^{-1}) carbonyl vibrations of 4 cm^{-1} for CNF, 12 cm^{-1} for alginate, and 7 cm^{-1} for the composite when calcium ions were introduced.

The suggested cooperation between alginate and CNF/CNC is based on the FTIR shift of the carbonyl peak position as a consequence of the calcium ions.[46] However, in the FTIR studies, the individual contributions from CNF and alginate to the total shift in the vibrations have not been taken into consideration. The previous claim[46] was based on TEMPO-oxidized cellulose and in this work carboxymethylated cellulose with a structure less similar to that of the alginate was used. Strong interactions with multivalent ions in the coordination bonds change the vibration energies for carboxylate groups and this shifts the asymmetric vibration, usually to lower wavenumbers, and the symmetric vibration, usually to higher wavenumbers for the bidentate (chelate) or bridging coordination (Fig. 7a).[20,79] The band-narrowing of 7 cm^{-1} for the CNF and alginate composite in Table 2 suggests a proportional combination of alginate and CNF ($0.3 \times 12 + 0.7 \times 4 = 6.4$ cm^{-1}) rather than a cooperative ion coordination. On the other hand, the relative amount of coordination bonds would probably be more or less maintained if a few carboxylate groups on CNF joins the egg-box structure, and might not be resolved with this technique.

The calcium-treated pristine CNF shows that no higher level coordination is present, since the vibration is almost the same in the sodium and calcium forms, which suggests that the mechanism for the wet-integrity of multivalent ions in nanopapers either gives a too low signal to be resolved by FTIR or is something other than the suggested ion coordination.[35,46] The wet integrity of pristine nanopapers with multivalent ions has been maintained with both carboxymethylated cellulose in the present work and TEMPO-oxidized CNF,[35–37] which strongly suggests that the CNF-calcium mechanism is not based on a specific geometry.

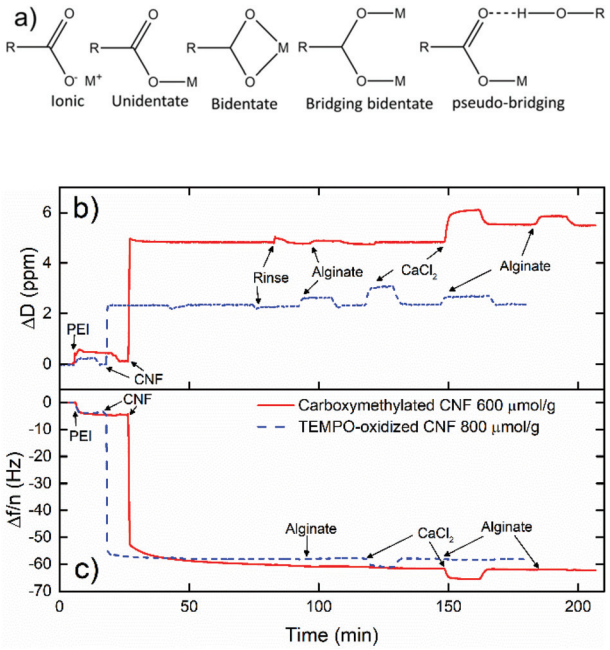

Fig. 7 (a) Ion coordination modes (denticity) between the carboxylic acids and metal ions and (b–c) QCM-D data of the third overtone showing the lack of interaction between alginate and CNF. (b) is the dissipation shift and (c) is the frequency shift.

A quartz crystal microbalance with dissipation was used to further investigate the interaction between CNF and alginate. Fig. 7b shows the build-up of a bilayer of PEI and carboxymethylated or TEMPO-oxidized CNF that was exposed to alginate when the cellulose surfaces were in the sodium or calcium form. The data show that alginate is unable to interact with the cellulose surfaces regardless of the counter-ion for cellulose which indicate that the repulsion from the electrical double layer is stronger than any other interactions. This does not, however, rule out the possibility that interactions are able to develop in the presence of calcium when CNF and alginate are forced into proximity during drying.

Suggested mechanism for attractive CNF interactions in the presence of multivalent ions

The FTIR data in Table 2 suggests that there is no high level of ion coordination for CNF, and this further indicates that there

Table 2 Asymmetric (ν_{asym}) and symmetric (ν_{sym}) carboxylate vibrations, peak separation ($\Delta\nu$), shift between the sodium and calcium states ($\Delta\Delta\nu$), and the denticity (Fig. 7a) of the interaction with sodium and calcium ions

Sample	$\nu_{asym}(COO^-)$	$\nu_{sym}(COO^-)$	$\Delta\nu$	$\Delta\Delta\nu$	Denticity[20] (Fig. 7a)
CNF Na^+	1594	1426	168		Ionic
CNF Ca^{2+}	1590	1426	164	−4	Ionic
Alginate Na^+	1592	1405	187		Ionic
Alginate Ca^{2+}	1586	1411[a]	175	−12	Pseudo-bridging[79]
CNF : Alginate 70 : 30 Na^+	1599	1418	181		Ionic
CNF : Alginate 70 : 30 Ca^{2+}	1595	1421[a]	174	−7	Ionic/pseudo-bridging

[a] The symmetric vibration is shifted to higher wavenumbers.

must be another explanation for the attractive force between CNF in the presence of calcium ions. In the early 70s, Oosawa introduced the concept of fluctuating counter-ion density close to a charged surface, *i.e.* the counter-ion concentration is not uniform outside the surface, which is not considered in the mean-field approximation in the DLVO theory.[38] The fluctuations are not only affected by external electrical fields but are also generated by thermal energy (kT) so that they are not negligible under ambient conditions. When two equally charged surfaces are forced together, the DLVO theory predicts a repulsive force between the surfaces due to the osmotic pressure of the overlapping counter-ion clouds, but in reality the ion density fluctuations can polarize the counter-ion cloud which leads to an attractive correlation force similar to the dispersive force generated by fluctuating electron densities (van der Waals). During the 1980s, Wennerström, Jönsson, and Kjellander with co-workers extended the theory they now call ion–ion correlation and also introduced the concept of image charges similar to an induced dipole-induced dipole (Debye) interaction, which in combination with the ion–ion correlation increased the attractive force even further.[39–41] The ion–ion correlation is low for monovalent ions and will not reverse the colloidal stability even in a highly charged system, but the exchange to multivalent ions in combination with high surface charge densities can lead to significant attraction between the surfaces at a short distance due to substantial deviations from the mean-field approximation in the DLVO theory.

These interactions are not generally considered in the context of colloidal stability but, due to the prominent effect of multivalent ions in nanopapers, they should indeed be considered and their relative importance should be quantified. Evans and Wennerström also suggested that these interactions are the reason why clay does not swell with calcium counter-ions,[42] and the analogy between the layered sheets in clay and the layered structure of crystalline fibrils in a dense and dry nanopaper, shown in ESI Fig. S3,† is not far-fetched.

The short range of the proposed interactions between CNF in the presence of calcium ions would also explain why it is possible to change the counter-ions of dilute CNF dispersions into multivalent ions and still maintain colloidal stability,[80] probably because the CNF are not close enough for ion–ion correlation interactions to develop.

Alginate prevents fibril orientation

Strain-induced stiffening was observed in the wet samples as an upward bend of the strain–stress curve towards the failure point, and is most likely due to an increased orientation of the fibrils with increasing strain.[74] Fig. 8 shows the birefringence images of the samples between crossed polarizers during strain to different extents, and the full video can be found in the ESI video.† The color shift in Fig. 8 can be interpreted by a Michel-Lévy or Raith–Sørensen color chart,[65] but it is difficult to translate the color changes to a change in orientation in the present case since the thickness and hence the amount of the optically active material or "optical thickness" in a given position changed during the straining. This means that the color

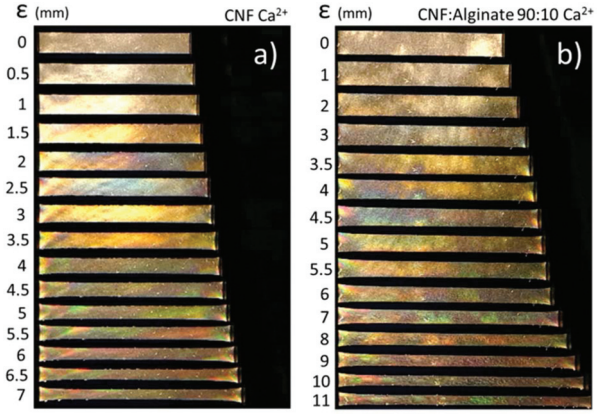

Fig. 8 Birefringence of (a) a calcium-treated nanopaper and (b) the calcium-treated composite with 10% alginate at different magnitudes of strain (ε) in the wet state. The samples were 20 mm long at zero strain and the final images (7 and 11) were taken just before failure.

shift is due to both a change in the "optical thickness", which affects the color at a given birefringence value, and to the alignment of the CNF. Qualitative interpretations can, however, be made based on the color change in Fig. 8 which shows distinct similarities and differences between the CNF and the composite sample. The initial color change was from white to yellow which can be observed for both samples in Fig. 8 and the ESI video,† but the strain at which this shift occurred differed significantly. For the CNF and the composite nanopaper, the yellow color appeared after strains of 1.5 and 3.5 mm, respectively, which suggests that the orientation is more easily achieved in the CNF sample without the alginate network. It can also be observed that the color was more even and more intense in the nanopaper than in the alginate composite that also split into different regions of orientation with indistinct colors. The CNF sample reached a second-order yellow color in the Michel-Lévy birefringence chart after 3 mm strain while the alginate composite had a marbled appearance with different colors after a strain of 4–4.5 mm. Towards the end of the test, both samples showed mixed regions with green or pink to a red color which is classified as a third or fourth order color in the Michel-Lévy birefringence chart.[65] Together, these observations lead to the suggestion that the alginate network prevents nanofibril orientation during strain, and also that it isolates different parts of the nanopaper so that each region aligns at an individual pace rather than collectively, as in the reference.

The described mechanism explains how the alginate network increases the stiffness and toughness of the composite by preventing the orientation of CNF into a deformed state where the CNF network starts to separate and the material fails. If this is the true mechanism, it means that the addition of only 10% alginate preserves the un-oriented CNF network at higher loads and greater extensions. It is also probable that the egg-box structure of the alginate is gradually unzipped[56] when the CNF network is forced towards higher degrees of orientation and that this process dissipates a lot of energy which in turn increases the toughness of the material.

These observations and suggestions mean that the material can be compared to a double network hydrogel with alginate as the tight and brittle sacrificial network that can dissipate energy and CNF as the long-distance load-transferring network that provides toughness, similar to the mechanism of the double network hydrogel of alginate and polyacrylamide (PAM) reported by Sun *et al.*[56] The difference is that the size of the CNF and of the mesh that it forms is not as uniform and flexible as that of the polymeric double network, and this can be a huge advantage given the right application.

Importance of how the interpenetrating networks are formed

Both the wet (Fig. 4) and dry (Fig. 5) mechanical properties of the nanopaper with 10% alginate suggest that optimal networks are formed when the dried composites are post-treated with Ca^{2+}. This is probably because the most efficient combination of the constituents forms the toughest interpenetrating networks.

In order to evaluate the importance of the interpenetrating networks, an experiment was designed where the alginate network was formed while the CNF was in a swollen state with a lot of voids between physically locked fibrils. This was achieved by swelling the never-dried composite film in Milli-Q water as in Fig. 3d and then introducing calcium ions in this state, illustrated in Fig. 9b, rather than into the collapsed dry film (Fig. 9a). The wet mechanical properties of this material were inferior even to the CNF reference, which indicates that the state in which the networks are formed by the introduction of counter-ions is vital (Fig. 9c). In this case, the alginate network was adapted to the swollen state, and would later be collapsed and have little influence on the material properties when the CNF network was formed during drying. The same trend was observed with a reference nanopaper when the calcium was introduced in the swollen gel state, and this suggests that proximity is crucial for the crosslinking mechanism for CNF using multivalent ions.

The 10% alginate composite in which the alginate network was formed in the swollen state showed a greater relative swelling thickness of 5.9, compared to 4.8 for the similarly treated reference nanopaper. This and the more drastic relative reduction in the stiffness and extensibility, compared to that in the composite crosslinked in the dry state, show that the influence of the alginate was more or less removed when a network adapted for the swollen gel state was formed (Fig. 9b).

Hygroplastic forming

The impressive extensibility and the high degree of plastic deformation of the composite with 10% alginate were utilized to press the film in the wet state into quite advanced hemispherical shapes, as shown in Fig. 10. The pressed film could later be freely dried on the bench while maintaining the forced shape. This opens up a new processing route that can be termed hygroplastic forming, and in this way it is possible to form advanced shapes with a water-resistant material with excellent gas barrier properties which is one step closer to a 100% bio-based and biodegradable alternative to thermoplastic packaging materials.

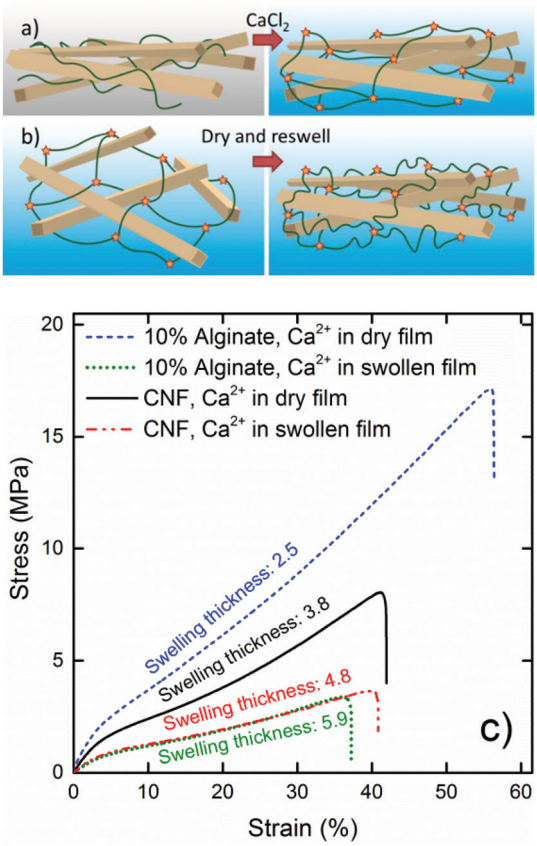

Fig. 9 A schematic illustration and tensile data of the interpenetrating networks formed with different treatments showing: (a) composite crosslinked from the dry state, (b) composite crosslinked in the swollen gel state that was dried and re-swollen before tensile testing, and (c) how these different treatments affect the mechanical properties in the wet state. The stars in (a) and (b) represent the crosslinking nodes.

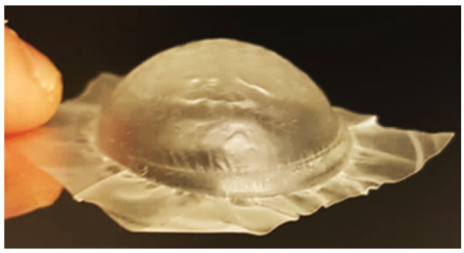

Fig. 10 The composite containing 90% CNF and 10% alginate by weight crosslinked with calcium ions, pressed in the wet state to form a hemispherical shape, and then freely dried under ambient conditions.

Conclusions

The sensitivity to water of most biomaterials limits their suitability for many material applications where plastics are used

today. In this work, an algae mimicking approach was adapted in order to remove or at least greatly reduce the sensitivity to water of nanopapers prepared from carboxymethylated cellulose nanofibrils. It was shown that 10 wt% alginate was sufficient to form an interpenetrating network that locked the CNF network into a tough material in the presence of calcium ions. The rigid alginate network was more efficient than the softer carrageenan network. The material was comparable to a high density double network hydrogel with calcium alginate as a sacrificial network and the nanofibrils locked by calcium ions as the long-range load-transfer network. The birefringence development due to fibril orientation during loading was greatly affected by the alginate, which suggests that the alginate network prevented the CNF from aligning and thus creating a more ductile material in both the dry and the wet state. The locking of CNF with Ca^{2+} was further investigated and it is suggested that it is an effect of ion–ion correlation forces generated by fluctuations in the counter-ion cloud in combination with image charges.

With the double network geometry, it was possible to form a material with a modulus of 135 MPa, a tensile strength of 17 MPa, a strain-at-break above 55%, and a work of fracture approaching 5 MJ m^{-3} in the wet state. The treatment also improved the dry tensile properties of the material with a modulus of 10.5 GPa, a tensile strength above 300 MPa, a strain-at-break approaching 12%, and a work of fracture of 25 MJ m^{-3}. The gas barrier properties were maintained to a greater extent at high relative humidity and the flexibility in the wet state allowed for hygroplastic forming into more advanced shapes, which is promising for future packaging applications.

Conflicts of interest

There are no conflicts of interest to declare.

Acknowledgements

The Wallenberg Wood Science Center (WWSC) and the Knut and Alice Wallenberg foundation are gratefully acknowledged for their financial support. Martin Sterner is acknowledged for his help with the alginate characterization. Per Larsson is acknowledged for his help with the hygroplastic forming.

References

1 G. Nystrom, A. Marais, E. Karabulut, L. Wagberg, Y. Cui and M. M. Hamedi, *Nat. Commun.*, 2015, **6**, 7259.
2 M. Wang, I. V. Anoshkin, A. G. Nasibulin, J. T. Korhonen, J. Seitsonen, J. Pere, E. I. Kauppinen, R. H. A. Ras and O. Ikkala, *Adv. Mater.*, 2013, **25**, 2428–2432.
3 F. Hoeng, A. Denneulin and J. Bras, *Nanoscale*, 2016, **8**, 13131–13154.
4 M. M. Hamedi, A. Hajian, A. B. Fall, K. Håkansson, M. Salajkova, F. Lundell, L. Wågberg and L. A. Berglund, *ACS Nano*, 2014, **8**, 2467–2476.
5 A. Liu, A. Walther, O. Ikkala, L. Belova and L. A. Berglund, *Biomacromolecules*, 2011, **12**, 633–641.
6 O. Köklükaya, F. Carosio and L. Wågberg, *ACS Appl. Mater. Interfaces*, 2017, **9**, 29082–29092.
7 N. Mittal, R. Jansson, M. Widhe, T. Benselfelt, K. M. O. Håkansson, F. Lundell, M. Hedhammar and L. D. Söderberg, *ACS Nano*, 2017, **11**, 5148–5159.
8 M. J. Lundahl, V. Klar, L. Wang, M. Ago and O. J. Rojas, *Ind. Eng. Chem. Res.*, 2017, **56**, 8–19.
9 K. Oksman, Y. Aitomäki, A. P. Mathew, G. Siqueira, Q. Zhou, S. Butylina, S. Tanpichai, X. Zhou and S. Hooshmand, *Composites, Part A*, 2016, **83**, 2–18.
10 L. A. Berglund and T. Peijs, *MRS Bull.*, 2011, **35**, 201–207.
11 F. L. Hatton, J. Engstrom, J. Forsling, E. Malmstrom and A. Carlmark, *RSC Adv.*, 2017, **7**, 14947–14958.
12 A. B. Fall, S. B. Lindström, O. Sundman, L. Ödberg and L. Wågberg, *Langmuir*, 2011, **27**, 11332–11338.
13 M. Nordenström, A. Fall, G. Nyström and L. Wågberg, *Langmuir*, 2017, **33**, 9772–9780.
14 A. B. Fall, A. Burman and L. Wagberg, *Nord. Pulp Pap. Res. J.*, 2014, **29**, 176–184.
15 T. Saito, S. Kimura, Y. Nishiyama and A. Isogai, *Biomacromolecules*, 2007, **8**, 2485–2491.
16 C. A. Steginsky, J. M. Beale, H. G. Floss and R. M. Mayer, *Carbohydr. Res.*, 1992, **225**, 11–26.
17 D. A. Rees and E. J. Welsh, *Angew. Chem., Int. Ed. Engl.*, 1977, **16**, 214–224.
18 G. W. Gokel, W. M. Leevy and M. E. Weber, *Chem. Rev.*, 2004, **104**, 2723–2750.
19 S. J. Angyal, *Adv. Carbohydr. Chem. Biochem.*, 1989, **47**, 1–43.
20 M. Nara, H. Morii and M. Tanokura, *Biochim. Biophys. Acta*, 2013, **1828**, 2319–2327.
21 A. Haug, B. Larsen and O. Smidsrød, *Acta Chem. Scand.*, 1966, **20**, 183–190.
22 G. T. Grant, E. R. Morris, D. A. Rees, P. J. C. Smith and D. Thom, *FEBS Lett.*, 1973, **32**, 195–198.
23 B. T. Stokke, O. Smidsrød, F. Zanetti, W. Strand and G. Skjåk-Bræk, *Carbohydr. Polym.*, 1993, **21**, 39–46.
24 R. Kohn and B. Larsen, *Acta Chem. Scand.*, 1972, **26**, 2455–2468.
25 W. Mackie, S. Perez, R. Rizzo, F. Taravel and M. Vignon, *Int. J. Biol. Macromol.*, 1983, **5**, 329–341.
26 L. Li, Y. Fang, R. Vreeker, I. Appelqvist and E. Mendes, *Biomacromolecules*, 2007, **8**, 464–468.
27 I. Donati, S. Holtan, Y. A. Mørch, M. Borgogna and M. Dentini, *Biomacromolecules*, 2005, **6**, 1031–1040.
28 E. R. Morris, D. A. Powell, M. J. Gidley and D. A. Rees, *J. Mol. Biol.*, 1982, **155**, 507–516.
29 A. Nussinovitch, in *Hydrocolloid Applications: Gum technology in the food and other industries*, Springer US, Boston, MA, 1997, pp. 40–62, DOI: 10.1007/978-1-4615-6385-3_3.

30 D. S. Reid, T. A. Bryce, A. H. Clark and D. A. Rees, *Faraday Discuss. Chem. Soc.*, 1974, **57**, 230–237.
31 S. Nilsson and L. Piculell, *Macromolecules*, 1991, **24**, 3804–3811.
32 E. R. Morris, D. A. Rees and G. Robinson, *J. Mol. Biol.*, 1980, **138**, 349–362.
33 M. Takemasa, A. Chiba and M. Date, *Macromolecules*, 2001, **34**, 7427–7434.
34 P. Agulhon, V. Markova, M. Robitzer, F. Quignard and T. Mineva, *Biomacromolecules*, 2012, **13**, 1899–1907.
35 M. Shimizu, T. Saito and A. Isogai, *J. Membr. Sci.*, 2016, **500**, 1–7.
36 H. Dong, J. F. Snyder, K. S. Williams and J. W. Andzelm, *Biomacromolecules*, 2013, **14**, 3338–3345.
37 K. S. Williams, J. W. Andzelm, H. Dong and J. F. Snyder, *Cellulose*, 2014, **21**, 1091–1101.
38 F. Oosawa, in *Polyelectrolytes*, Marcel Dekker, 1971.
39 L. Guldbrand, B. Jönsson, H. Wennerström and P. Linse, *J. Chem. Phys.*, 1984, **80**, 2221–2228.
40 R. Kjellander and S. Marčelja, *Chem. Phys. Lett.*, 1984, **112**, 49–53.
41 D. Bratko, B. Jönsson and H. Wennerström, *Chem. Phys. Lett.*, 1986, **128**, 449–454.
42 D. F. Evans and H. Wennerström, *The Colloidal Domain: Where Physics, Chemistry, Biology, and Technology Meet*, Wiley-Vch, 2nd edn, 1999.
43 A. Nussinovitch, in *Hydrocolloid Applications: Gum technology in the food and other industries*, Springer US, Boston, MA, 1997, pp. 19–39, DOI: 10.1007/978-1-4615-6385-3_2.
44 J. D. Kittle, X. Du, F. Jiang, C. Qian, T. Heinze, M. Roman and A. R. Esker, *Biomacromolecules*, 2011, **12**, 2881–2887.
45 N. Naseri, B. Deepa, A. P. Mathew, K. Oksman and L. Girandon, *Biomacromolecules*, 2016, **17**, 3714–3723.
46 N. Lin, C. Bruzzese and A. Dufresne, *ACS Appl. Mater. Interfaces*, 2012, **4**, 4948–4959.
47 J. A. Sirviö, A. Kolehmainen, H. Liimatainen, J. Niinimäki and O. E. O. Hormi, *Food Chem.*, 2014, **151**, 343–351.
48 K. Markstedt, A. Mantas, I. Tournier, H. Martínez Ávila, D. Hägg and P. Gatenholm, *Biomacromolecules*, 2015, **16**, 1489–1496.
49 D. Gomez-Martinez, M. Stading and A.-M. Hermansson, *Annual Transactions of the Nordic Rheology Society*, 2012, vol. 20, pp. 117–121.
50 Q. Lin, Y. Zheng, L. Ren, J. Wu, H. Wang, J. An and W. Fan, *J. Appl. Polym. Sci.*, 2014, **131**, 39848.
51 T. Huq, S. Salmieri, A. Khan, R. A. Khan, C. Le Tien, B. Riedl, C. Fraschini, J. Bouchard, J. Uribe-Calderon, M. R. Kamal and M. Lacroix, *Carbohydr. Polym.*, 2012, **90**, 1757–1763.
52 E. E. Ureña-Benavides, P. J. Brown and C. L. Kitchens, *Langmuir*, 2010, **26**, 14263–14270.
53 Y. Qin, *Polym. Int.*, 2008, **57**, 171–180.
54 Q. Chen, H. Chen, L. Zhu and J. Zheng, *J. Mater. Chem. B*, 2015, **3**, 3654–3676.
55 J. P. Gong, *Soft Matter*, 2010, **6**, 2583–2590.
56 J.-Y. Sun, X. Zhao, W. R. K. Illeperuma, O. Chaudhuri, K. H. Oh, D. J. Mooney, J. J. Vlassak and Z. Suo, *Nature*, 2012, **489**, 133–136.
57 M. S. Toivonen, S. Kurki-Suonio, F. H. Schacher, S. Hietala, O. J. Rojas and O. Ikkala, *Biomacromolecules*, 2015, **16**, 1062–1071.
58 L. Wågberg, G. Decher, M. Norgren, T. Lindström, M. Ankerfors and K. Axnäs, *Langmuir*, 2008, **24**, 784–795.
59 H. Grasdalen, B. Larsen and O. Smidsrød, *Carbohydr. Res.*, 1979, **68**, 23–31.
60 E. Tojo and J. Prado, *Carbohydr. Polym.*, 2003, **53**, 325–329.
61 F. van de Velde and H. S. Rollema, in *Modern Magnetic Resonance*, ed. G. A. Webb, Springer Netherlands, Dordrecht, 2006, pp. 1605–1610, DOI: 10.1007/1-4020-3910-7_178.
62 A. Pantze, O. Karlsson and U. Westermark, *Holzforschung*, 2008, **62**, 136–141.
63 K. A. Marx, *Biomacromolecules*, 2003, **4**, 1099–1120.
64 T. Saito, M. Hirota, N. Tamura, S. Kimura, H. Fukuzumi, L. Heux and A. Isogai, *Biomacromolecules*, 2009, **10**, 1992–1996.
65 B. E. Sørensen, *Eur. J. Mineral.*, 2013, **25**, 5–10.
66 P. A. Larsson, L. A. Berglund and L. Wågberg, *Biomacromolecules*, 2014, **15**, 2218–2223.
67 J. Kötz and T. Beitz, *Trends Polym. Sci.*, 1997, **5**(3), 86–90.
68 R. F. Shamoun, A. Reisch and J. B. Schlenoff, *Adv. Funct. Mater.*, 2012, **22**, 1923–1931.
69 P. J. Flory, *Principles of Polymer Chemistry*, Cornell University Press, 1953.
70 S. Takaichi, T. Saito, R. Tanaka and A. Isogai, *Cellulose*, 2014, **21**, 4093–4103.
71 S. Nilsson and L. Piculell, *Macromolecules*, 1989, **22**, 3011–3017.
72 M. Tako and S. Nakamura, *Carbohydr. Res.*, 1986, **155**, 200–205.
73 M. Tako, S. Nakamura and Y. Kohda, *Carbohydr. Res.*, 1987, **161**, 247–255.
74 H. Sehaqui, N. Ezekiel Mushi, S. Morimune, M. Salajkova, T. Nishino and L. A. Berglund, *ACS Appl. Mater. Interfaces*, 2012, **4**, 1043–1049.
75 S. Liu, J. Ling, K. Li, F. Yao, O. Oderinde, Z. Zhang and G. Fu, *RSC Adv.*, 2016, **6**, 63171–63177.
76 A. Walther and A. Benitez, *J. Mater. Chem. A*, 2017, **5**, 16003–16024.
77 P. A. Larsson, T. Pettersson and L. Wågberg, *Green Mater.*, 2014, **2**, 163–168.
78 İ. Özen, G. Bozoklu, C. Dalgıçdir, O. Yücel, E. Ünsal, M. Çakmak and Y. Z. Menceloğlu, *Eur. Polym. J.*, 2010, **46**, 226–237.
79 S. K. Papageorgiou, E. P. Kouvelos, E. P. Favvas, A. A. Sapalidis, G. E. Romanos and F. K. Katsaros, *Carbohydr. Res.*, 2010, **345**, 469–473.
80 A. Sone, T. Saito and A. Isogai, *ACS Macro Lett.*, 2016, **5**, 1402–1405.

